Bioinformatics analysis of the structural and evolutionary characteristics for toll-like receptor 15

Jinlan Wang[1], Zheng Zhang[2], Fen Chang[1] and Deling Yin[3,4]

[1] Institute of Developmental Biology, School of Life Science, Shandong University, Jinan, China
[2] State Key Laboratory of Microbial Technology, School of Life Science, Shandong University, Jinan, China
[3] School of Pharmacy, Central South University, Changsha, China
[4] Department of Internal Medicine, College of Medicine, East Tennessee State University, Johnson, TN, USA

ABSTRACT

Toll-like receptors (TLRs) play important role in the innate immune system. TLR15 is reported to have a unique role in defense against pathogens, but its structural and evolution characterizations are still poorly understood. In this study, we identified 57 completed TLR15 genes from avian and reptilian genomes. TLR15 clustered into an individual clade and was closely related to family 1 on the phylogenetic tree. Unlike the TLRs in family 1 with the broken asparagine ladders in the middle, TLR15 ectodomain had an intact asparagine ladder that is critical to maintain the overall shape of ectodomain. The conservation analysis found that TLR15 ectodomain had a highly evolutionarily conserved region on the convex surface of LRR11 module, which is probably involved in TLR15 activation process. Furthermore, the protein–protein docking analysis indicated that TLR15 TIR domains have the potential to form homodimers, the predicted interaction interface of TIR dimer was formed mainly by residues from the BB-loops and αC-helixes. Although TLR15 mainly underwent purifying selection, we detected 27 sites under positive selection for TLR15, 24 of which are located on its ectodomain. Our observations suggest the structural features of TLR15 which may be relevant to its function, but which requires further experimental validation.

Subjects Bioinformatics, Immunology

Keywords Toll-like receptor 15, Innate immunity, Structural characteristics, Protein–protein interactions, Molecular evolution

Submitted 26 February 2016
Accepted 3 May 2016
Published 25 May 2016

Corresponding authors
Zheng Zhang, zhzhang.sdu@gmail.com
Deling Yin, delingyin@yahoo.com

Academic editor
Fulvio D'Acquisto

Additional Information and Declarations can be found on page 12

DOI **10.7717/peerj.2079**

INTRODUCTION

Innate immunity stands on the first line of immune defense against pathogens. Toll-like receptors (TLRs) are a major class of pattern recognition receptors in innate immunity, they recognize a variety of highly conserved pathogen-associated molecular patterns (PAMPs) in pathogens to initiate an innate immune response and prime the adaptive immune system (*Akira & Takeda, 2004*). TLR is characterized by the presence of an ectodomain that is involved in recognizing ligands and an intracellular Toll/IL-1 receptor-like (TIR) domain that mediates signaling (*Kang & Lee, 2011*). The ectodomain of TLR contains a large number of leucine-rich repeat (LRR) modules and is generally bent into a characteristic horseshoe-shaped structure (*Botos, Segal & Davies, 2011*).

So far, 27 types of TLRs have been identified in vertebrates (*Wang et al., 2015a*; *Wang et al., 2015b*), the ligand specificities of some TLRs have been clarified. TLR2 is able to form a heterodimer with TLR1, TLR6 or TLR10 to detect microbial lipopeptides (*Guan et al., 2010*; *Jin et al., 2007*; *Kang et al., 2009*); TLR3 and TLR22 detect double-stranded RNA (*Liu et al., 2008*; *Matsuo et al., 2008*); TLR4 recognizes to lipopolysaccharides from Gram-negative bacteria (*Park et al., 2009*); TLR5 binds to bacterial flagellin (*Yoon et al., 2012*); TLR7, TLR8, and TLR13 bind to single-stranded RNA (*Heil et al., 2004*; *Shi et al., 2011*; *Tanji et al., 2015*), TLR9 and TLR21 recognize unmethylated CpG-containing DNA (*Brownlie et al., 2009*; *Keestra et al., 2010*; *Ohto et al., 2015*; *Yeh et al., 2013*), and TLR11 and TLR12 respond to profilin (*Koblansky et al., 2013*; *Yarovinsky et al., 2005*).

TLR15 can be identified in avian and some reptilian species (*Alcaide & Edwards, 2011*; *Boyd et al., 2012*). TLR15 was considered to play a constitutive role in the immune defense of chickens (*Higgs et al., 2006*). The expression of TLR15 was strongly up-regulated after *Salmonella enterica* infection (*Higgs et al., 2006*; *Hu et al., 2016*; *Shaughnessy et al., 2009*). TLR15 was reported to have a unique activation mechanism, where the cleavage of TLR15 ectodomain by secreted microbial proteases results in its activation (*De Zoete et al., 2011*). A later study showed that TLR15 recognized a yeast-derived agonist that was heat labile and inhibited by PMSF (*Boyd et al., 2012*). The diacylated lipopeptide from *Mycoplasma synoviae* was reported to mediate TLR15-dependent innate immune responses (*Oven et al., 2013*).

Benefiting from the recently rapid increasing of genome data, a large number of TLR sequences are determined (*Zhang et al., 2014*). In the current work, we identified 57 completed TLR15 genes from the genomes in vertebrates, investigated the phylogenetic relationships, structural and evolutionary characterizations using these sequences, and predicted the dimeric interaction of TLR15 TIR domains.

MATERIALS AND METHODS

Phylogenetic analysis

The coding sequences of vertebrate TLR genes were retrieved from NCBI (GenBank) and Ensembl databases (*Benson et al., 2013*; *Cunningham et al., 2015*). All the partial sequences (<1,800 bp) and pseudogene sequences were excluded. A multiple sequence alignment of the TLR proteins was constructed with MAFFT (FFT-NS-i, BLOSUM62) (*Katoh & Standley, 2013*), and a phylogenetic tree was calculated from it with PhyML using the LG substitution model and four substitution rate categories (*Guindon et al., 2010*; *Le & Gascuel, 2008*). Branch support was calculated with an approximate likelihood ratio tests (aLRT SH-like) (*Anisimova & Gascuel, 2006*). The phylogenetic tree was visualized with MEGA 6 (*Tamura et al., 2013*).

Structural elements analysis

SignalP, SMART, and TMHMM were used to identify the signal peptide, ectodomain, transmembrane region, and intracellular TIR domain of TLR15 (*Krogh et al., 2001*; *Letunic, Doerks & Bork, 2015*; *Petersen et al., 2011*). The delimitation of each LRR module in the TLR15 ectodomain was determined with the LRRfinder software (*Offord, Coffey & Werling, 2010*). The delimitations of chicken TLR15 were used as the reference for the remaining species.

Structural modeling

I-TASSER was used to model the structure of the ectodomain and TIR domain of TLR15 based on a threading approach (*Yang et al., 2015*). I-TASSER is a hierarchical method for protein structure prediction. Structural templates were first identified from the PDB by the multiple-threading program LOMETS; then, full-length models were constructed by iterative template fragment assembly simulations. The modeled structure was displayed by PyMol (Schrödinger, LLC).

Protein–protein docking analysis

The two modeled structures of chicken TLR15 TIR domains were submitted as target 1 and target 2, respectively, to PRISM protein–protein docking server (*Baspinar et al., 2014*; *Tuncbag et al., 2011*). PRISM predicts possible interactions, and how the interaction partners connect structurally, based on geometrical comparisons of the template structures and the target structures.

Residue conservation analysis

A multiple sequence alignment of the TLR15 proteins was constructed with MAFFT. The evolutionary conservations of amino acid residue positions in the TLR15 sequences was estimated by using ConSurf algorithm (*Ashkenazy et al., 2010*). The JTT substitution matrix was used and computation was based on the empirical Bayesian paradigm. The conservation scale was defined from the most variable amino acid positions (grade 1) which were considered as rapidly evolving, to the most conservative amino acid positions (grade 9) which were considered as slowly evolving. The sequence and modeling structure of chicken TLR15 were used to show the nine-color conservation grades.

Codon-based analyses of positive selection

A multiple sequence alignment of the nucleic acid sequences of the *TLR15* genes, based on their codons, was established with TranslatorX (*Abascal, Zardoya & Telford, 2010*). The ratio of the number of nonsynonymous substitutions per nonsynonymous site (dN) to the number of synonymous substitutions per synonymous site (dS), dN/dS, an indicator of the selective pressure acting on a protein-coding gene, at the TLR15 locus and the corresponding 95% confidence interval were calculated with the Datamonkey web server (*Delport et al., 2010*).

The SLAC, FEL, REL, and FUBAR methods were implemented in Datamonkey to explore the evidence of positive selection acting on the individual codon of the *TLR15* sequences (*Kosakovsky Pond & Frost, 2005*; *Murrell et al., 2013*). To minimize the overestimation of the positively selected codons, codons with p values < 0.1 for SLAC and FEL, with Bayes Factor > 50 for REL, and with posterior probabilities > 0.9 for FUBAR were considered as candidates to be under positive selection.

RESULTS

TLR15 is phylogenetically closely related to family 1

We obtained all the known vertebrate full-length TLR gene sequences and constructed their phylogenetic relationships based on maximum likelihood method (Fig. 1A). TLR15

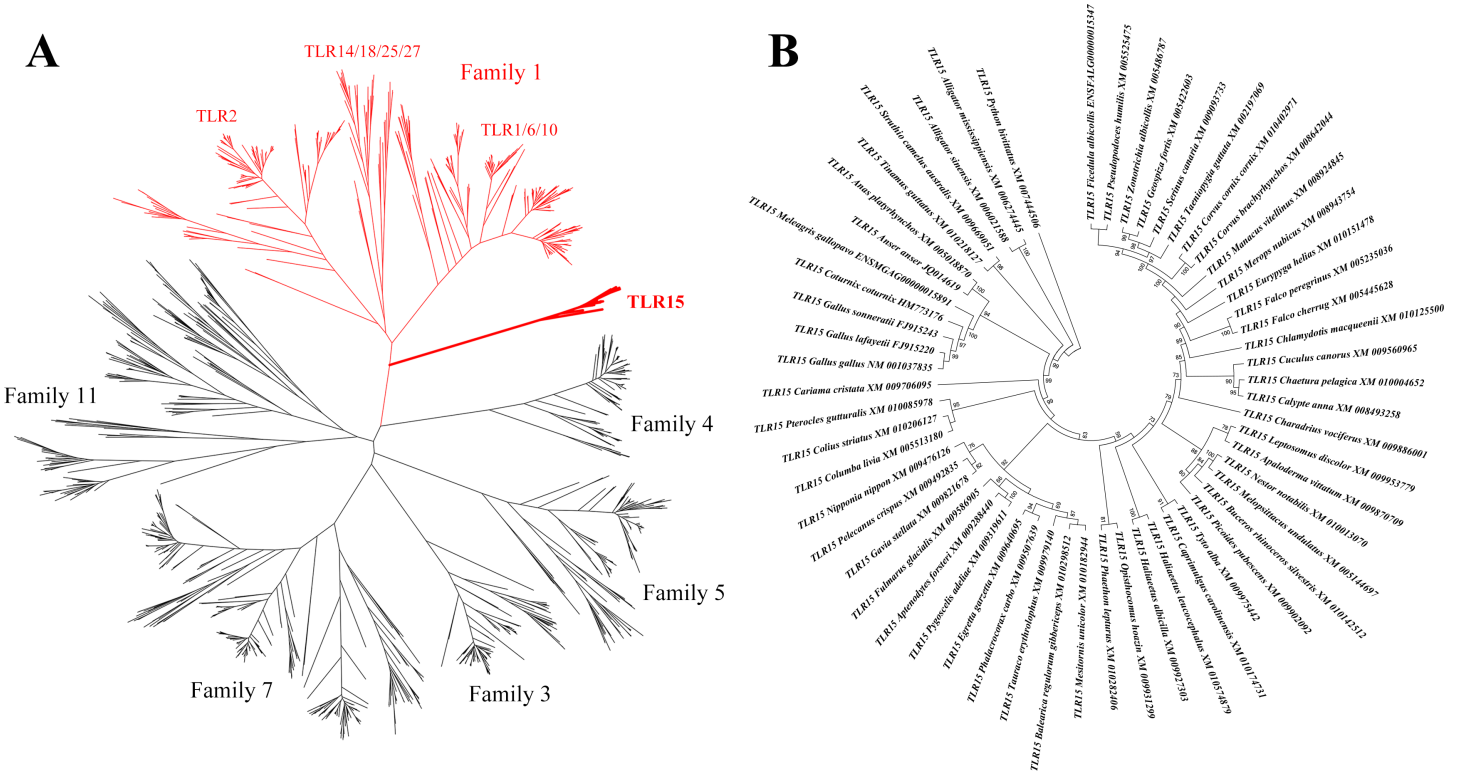

Figure 1 Phylogenetic analysis of TLR15 and the other vertebrate TLRs. (A) A large unrooted tree of all the known vertebrate TLRs. Maximum likelihood tree was constructed based on the full-length sequences of TLRs. Six TLR families are labeled in the tree. The clades of family 1 are shown in red and the clades of TLR15s are shown in bold. (B) Amplified TLR15 clades of the large unrooted tree. The support value at each branching point is shown. Its robustness was estimated with an aLRT SH-like method.

clusters into an individual clade and is closely related to the TLRs in family 1 (TLR1, TLR2, TLR6, TLR10, TLR14, TLR18, TLR25 and TLR27) on the phylogenetic tree. This is consistent with the early finding (*Roach et al., 2005*).

We identified 57 completed TLR15 genes through the phylogenetic analysis (Fig. 1B, Table S1). These TLR15 sequences are derived from 54 avian and 3 reptilian species (Burmese python, Chinese alligator, and American alligator). TLR15 exists in these species as a single gene copy in each species' genome. Also, the phylogenetic tree showed that TLR15 has evolved following the phylogeny of species. These results indicate that TLR15 is possibly subjected to strong selection constraints.

TLR15 ectodomain possesses an intact asparagine ladder

TLR15 generally include 860∼880 amino acids. Motif prediction showed that TLR15 included the signal peptide, ectodomain, transmembrane region, and intracellular TIR domain. The structure of chicken TLR15 ectodomain was modeled with threading approach (Fig. 2A). The estimated TM-score (0.72 ± 0.11) for this modeled structure showed that it was acceptable. TLR15 ectodomain contains a LRRNT, a LRRCT, and 19 LRR modules, which is identical to the number of LRR modules of the known TLRs in family 1. The LRR3

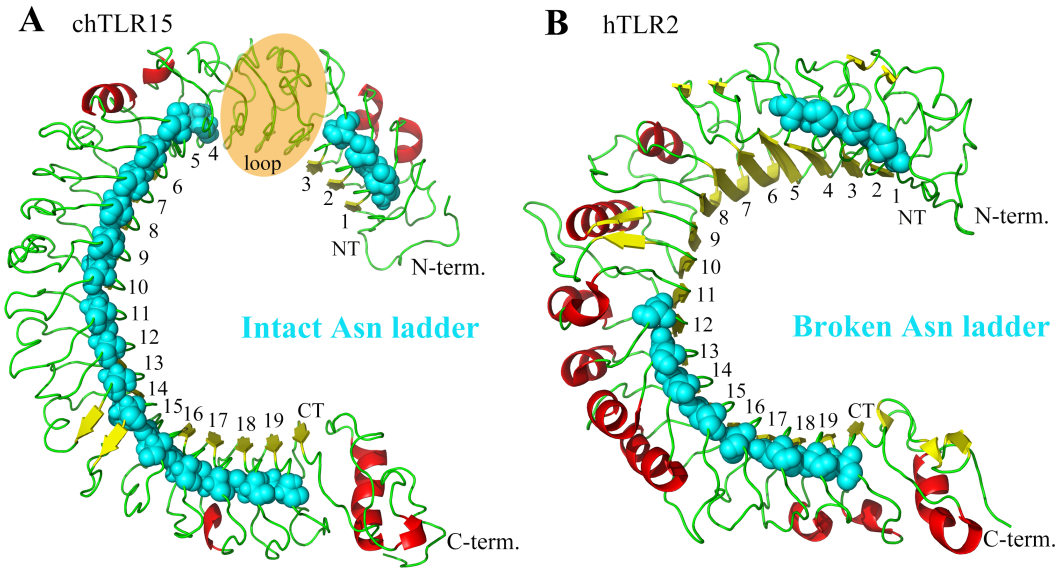

Figure 2 Comparison between the asparagine ladders in the ectodomains of TLR15 and the other TLRs in family 1. (A) TL15 has an intact asparagine ladder in the ectodomain. The model is chicken TLR15 ectodomain. There was a predicted long loop between LRR3 and LRR4 modules, in which the conserved "LxxLxLxxNxL" motif was not found. (B) The asparagine ladders of the other TLRs in family 1 are broken in the middle. The crystal structure of human TLR2 ectodomain (PDB code: 2Z7X) is displayed as an example. The ectodomain structures are shown in cartoon mode. The residues in the asparagine ladder position (cyan) are shown by sphere mode. The identifying numbers of the 19 canonical LRR, LRRNT and LRRCT modules are labeled.

module of TLR15 is quite long, for example, the LRR3 of chicken TLR15 has 99 amino acids that far exceed the lengths of common LRR modules (~24 amino acids).

The LRR module is characterized by a conserved "LxxLxLxxNxL" motif on the concave surface. Among them, the conserved asparagine plays important role in maintaining the overall shape of TLR ectodomain by forming a continuous hydrogen-bond network (called as asparagine ladder) with backbone carbonyl oxygens of neighboring LRR modules (*Kang & Lee, 2011*). The asparagines can be substituted by other amino acids that are able to donating hydrogens, such as threonine, serine, and cysteine. We analyzed the asparagine ladder in the ectodomain of TLR15. The results showed that the asparagine ladder was intact throughout the TLR15 ectodomain, suggesting that TLR15 possesses an intact and continuous hydrogen-bond network (Fig. 2A).

Although both TLR15 and the TLRs in family 1 contain 19 LRR modules, the known crystal structures indicate that the asparagine ladders of the ectodomains of TLRs in family 1 are broken in the middle (Fig. 2B). TLR15 ectodomain more approximates to those TLRs with intact asparagine ladders in the ectodomains, for example, TLR3, TLR5, TLR7, and TLR21 (Table S2). Therefore, the ectodomain of TLR15 is obviously structurally different from the TLRs in family 1.

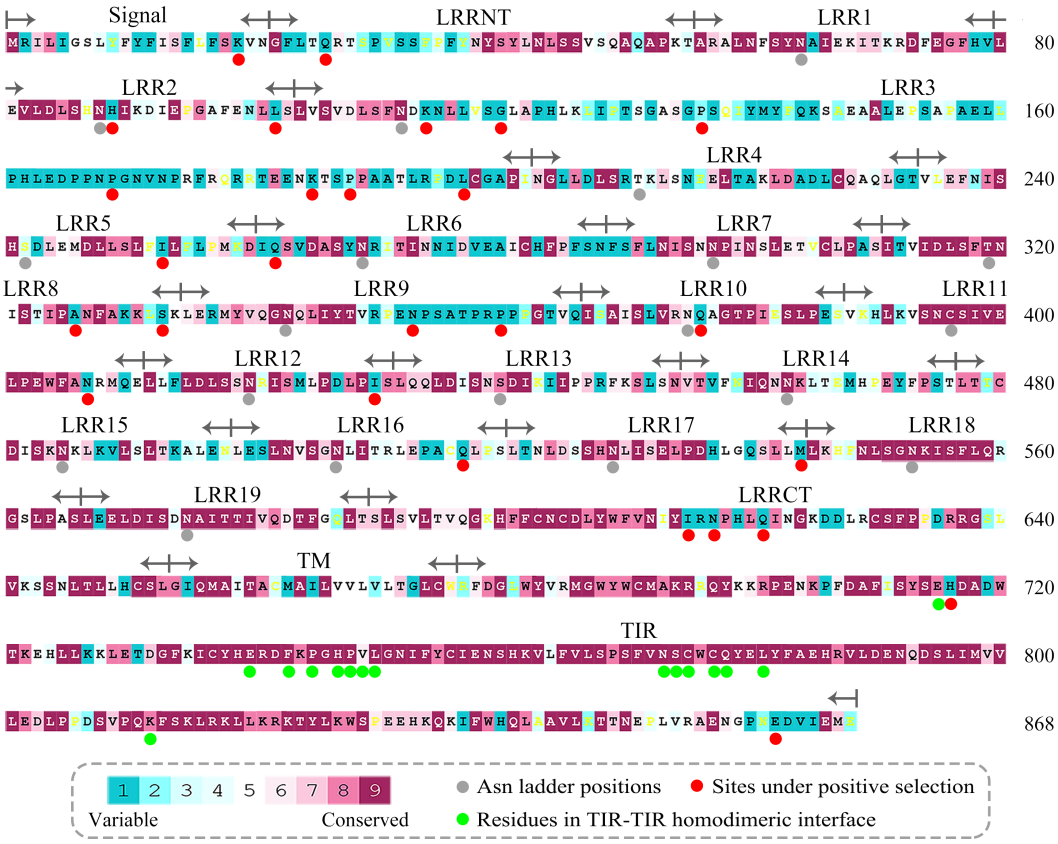

Figure 3 Evolutionary conservation s of amino acid positions displayed in the sequence of TLR15. The conservation scale was defined from the most variable amino acid positions (grade 1, colored turquoise) to the most conservative amino acid positions (grade 9, colored maroon). Positions, for which the inferred conservation level was assigned with low confidence, are marked with light yellow. The sequence of chicken TLR15 was used to show the nine-color conservation grades. The signal peptide, the predicted LRR modules of the ectodomain, transmembrane region (TM), and intracellular domain (TIR) for TLR15 are labeled. The residues in asparagine ladder positions in the concave surface of each LRR module, the sites under positive selection, and the residues involved in the homodimeric interaction of TLR15 TIR domains are marked with solid gray circles, solid red circles, and solid green circles under the sequence, respectively.

The convex surface of TLR15 ectodomain has a highly evolutionarily conserved region

We calculated the evolutionary conservation scores of all residue positions of TLR15 based on the phylogenetic relationships between homologous sequences (Fig. 3). The conservation scale was defined from the most variable amino acid positions, which were considered as rapidly evolving, to the most conservative amino acid positions, which were considered as slowly evolving. Further, the mean evolutionary conservation score of each module in TLR15 was also calculated (Fig. 4).

The results showed that the majority of amino acid positions of intracellular TIR domain were highly evolutionarily conserved. However, the average evolutionary conservation of different LRR module in the ectodomain had large differences. Most of LRR3 module was

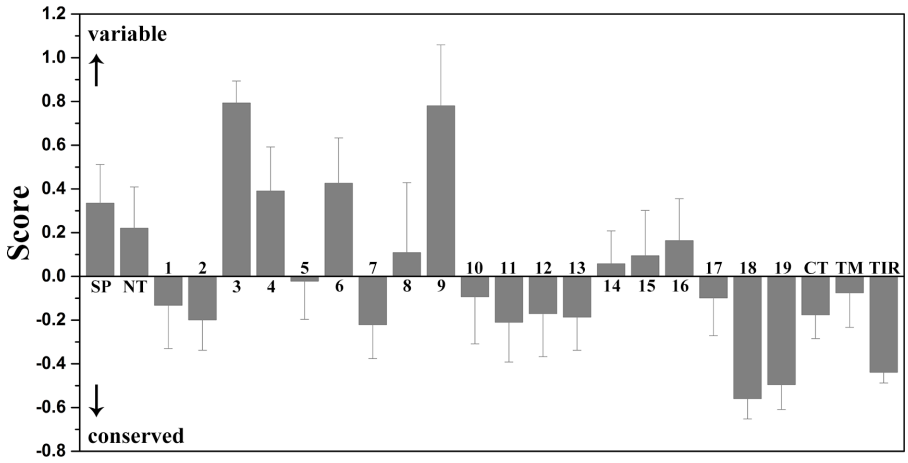

Figure 4 Mean evolutionary conservation of each module of TLR15. SP, Signal peptide; NT, LRRNT module; CT, LRRCT module; TM, transmembrane region; TIR, intracellular domain. The different LRR modules of the ectodomain are represented by their identifying numbers. The lowest score represents the most conserved position in a protein. The error bars represent the standard error of the mean (SEM).

composed of highly variable positions. The loop of convex surface in LRR9 module also includes a number of highly variable positions. The average evolutionary conservations of LRR18, LRR19, and LRRCT modules are very high, this could be adapted to their function participating in the dimerization of C-terminal region of TLR15 ectodomain. The average evolutionary conservations of LRR10-13 modules are also very high, indicating that they are possibly related to the function of the ectodomain sensing pathogens.

We further displayed the evolutionary conservations of amino acid residue positions in the ectodomain of TLR15 using the modeled structure (Fig. 5). The asparagine ladder with high evolutionary conservation is located on the ascending lateral surface, which contains loops connecting the β-strand of the concave surface to the convex surface and participates in the dimerization of TLRs (*Botos, Segal & Davies, 2011*). Compared to the ascending lateral surface, its opposite side, the descending lateral surface, includes fewer evolutionarily conserved positions. Interestingly, we found a highly conserved region on the convex surface of TLR15 ectodomain, which is exactly located on the LRR11 module. For chicken TLR15, the highly conserved region on the convex surface of its LRR11 module ranges from 397th to 406th amino acid residues (SIVELPEWFA). The high conservation of this region across species might suggest that it is involved in ligand recognition.

TLR15 TIR domains are able to form homodimers

We further studied TLR15 intracellular TIR domain that is responsible for the signal transduction. The structure of TIR domain (from Pro706 to Thr848) of chicken TLR15 was modeled with threading approach. This modeled structure mainly contains a central three-stranded parallel β-sheet surrounded by five α-helices (Fig. 6A).

Protein–protein docking analysis showed that TLR15 TIR domain was able to form the homodimer with itself (Fig. 6A). The dimeric interface is mainly formed by the residues from the BB-loops and αC-helixes. The fifteen residues of TLR15 TIR domain

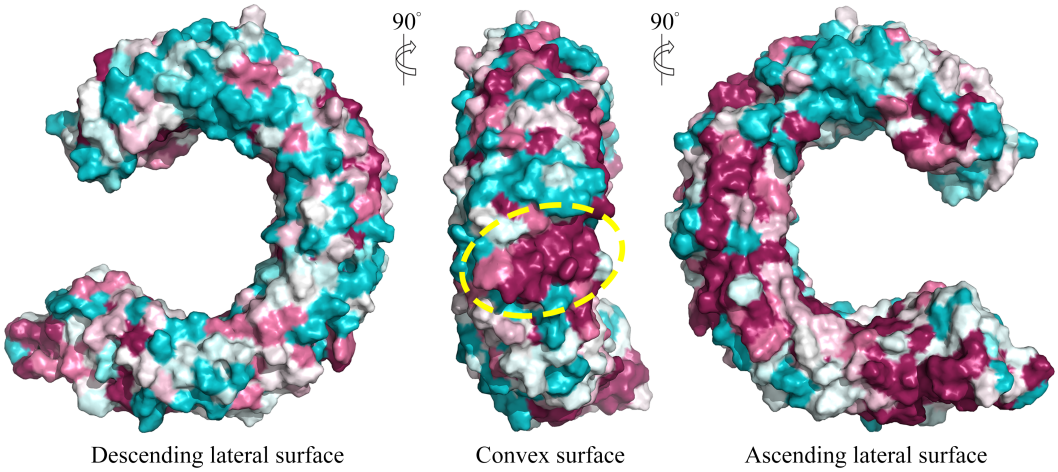

Figure 5 Surface evolutionary conservation of TLR15 ectodomain. A highly evolutionarily conserved region on the convex surface of TLR15 ectodomain is labeled with dashed yellow circle. The modeling structure of chicken TLR15 was used to show the conservation. The surfaces are colored according to ConSurf results: the most variable (turquoise) to the most conserved (maroon).

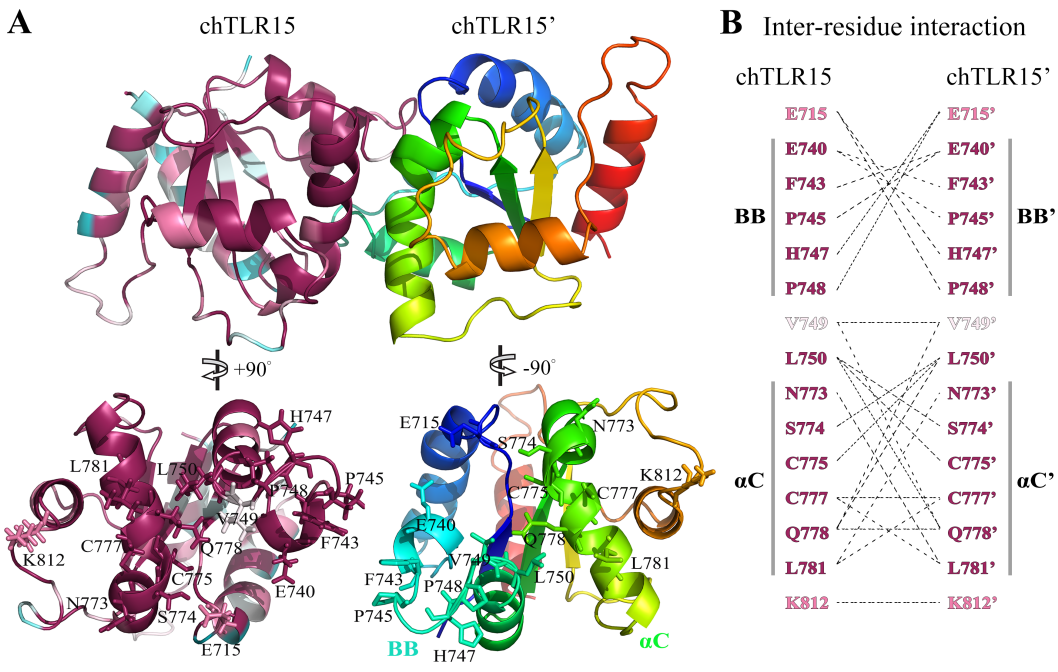

Figure 6 Prediction of TLR15 TIR domain homodimeric interaction. (A) Cartoon figure of TLR15 TIR homodimeric interaction predicted through docking calculations. The left monomeric structure is colored according to the conservation score of each residue position, while the N-terminus to the C-terminus of the right one is colored from blue to red. The homodimerization interface has been split and rotated to show the involved residues. (B) Inter-residues interaction in potential dimerization interfaces. The interaction partners are connected by broken lines. The modeled structure of chicken TLR15 TIR domain was used for docking analysis. The residues are numbered according to the chicken TLR15 sequence.

were predicted to participate in its homodimerization, the five of them are located on the BB-loops and six of them are located on the αC-helixes (Fig. 6B). Cys777 in αC-helix at one monomer (chTLR15) probably formed disulfide bond with the same residue from the second molecule (chTLR15'). The amino acid residue positions involved in the interaction of TIR homodimer are highly evolutionarily conserved among 57 TLR15 sequences (Fig. 6B). The fourteen of fifteen residue positions involved in the homodimeric interaction have an evolutionary conservation score greater than or equal to the grade 8.

We compared the predicted dimerization of TLR15 with those of the TLRs in family 1. The multiple sequence alignment showed that there were 30% identical amino acid residues among the TIR domains of chicken TLR15, human TLR1, human TLR2, human TLR6, and human TLR10 (Fig. 7). The known five functionally critical residues in TLR2 TIR domain are conserved among different TLRs (*Tao et al., 2002*), which correspond to Phe743, Pro745, Cys777, Leu781, and Lys812 in chicken TLR15. The homodimer interface of TLR6 TIR domains is considered to be formed mainly by the residues from αC-helixes (*Jang & Park, 2014*), the six of its eight interaction residues was also found in the interaction of TLR15 TIR domain homodimer. The homodimer interface of TLR10 TIR domains was reported to mainly contain residues from the BB-loops and αC-helixes (*Nyman et al., 2008*). The nine of its eleven interaction residues was also detected in the interaction of TLR15 TIR domain homodimer. Comparatively speaking, the interaction mode of TLR15 TIR homodimer is more similar to that of TLR10.

Twenty-seven sites under positive selection were detected for TLR15

The estimated *dN/dS* value for the *TLR15* locus is 0.318 (95% CI [0.308–0.328]), suggesting a clear excess of synonymous over nonsynonymous substitutions at *TLR15* locus. However, numerous sites under positive selection were found in *TLR15* with the codon-based maximum likelihood methods (Table 1). The SLAC, FEL, REL, and FUBAR methods identified statistically significant positive selection in 24, 29, 22, 14 amino acid sites across TLR15s, respectively. To identify robust candidate sites under positive selection, only 27 codons with evidence of positive selection identified by at least two methods were considered, which account for 3.1% of the total sites in TLR15.

These 27 sites under positive selection belong to the most variable positions identified by evolutionary conservation analysis (Fig. 3). The 24 of 27 sites under positive selection are located on TLR15 ectodomain. Among them, the LRR3 module contains seven sites under positive selection. The proline-rich loop on the convex surface of LRR9 module includes two sites under positive selection. There is also a site under positive selection (407th) closely neighboring to the highly evolutionarily conserved region on the convex surface of LRR11 module.

DISCUSSION

Although TLR15 is phylogenetically close to family 1, our modeling structure showed that TLR15 ectodomain was obviously structurally different from the TLRs in family 1. The known crystal structures indicate that the asparagine ladders in the ectodomains of TLRs in family 1 are broken in the middle, thus resulting in the structural transition

Figure 7 Alignment of representative TIR domain sequences from different TLRs. The surface residues involved in the homodimeric interaction detected by protein–protein docking analysis for TLR15 are shaded in green. The surface residues on TLR6 and TLR10 involved in TIR–TIR interaction are shaded in pink and yellow, respectively. The surface residues on TLR2 that have been known to be critical for the TLR signaling are shaded in light blue. The elements of secondary structures are labeled above the sequence. Consistent with the previous work of TIR domains, the loops are named by the strands and helices that they connect.

Table 1 Tests for positive selection of TLR15s.

Methods	Sites under positive selection[d]
SLAC[a]	19, 26, 33, 89, 102, 120, 136, 169, 188, 197, 253, 262, 283, 326, 333, 376, 407, 430, 517, 615, 617, 621, 716, 862
FEL[a]	19, 26, 89, 102, 114, 120, 136, 169, 185, 188, 197, 253, 262, 326, 333, 353, 360, 376, 407, 430, 517, 544, 597, 615, 617, 621, 643, 716, 862
REL[b]	89, 114, 120, 132, 169, 197, 253, 262, 333, 337, 376, 407, 410, 430, 452, 517, 544, 615, 617, 650, 655, 862
FUBAR[c]	26, 102, 136, 185, 197, 253, 326, 333, 353, 360, 430, 615, 617, 621

Notes.

[a]Codons with p values < 0.1.

[b]Codons with Bayes factor > 50.

[c]Codons with posterior probability > 0.9.

[d]Those positively selected sites identified by more than one method are underlined. Sites are numbered according to the chicken TLR15 sequence.

of their ectodomain in the middle, and further causing the formation of a hydrophobic pocket at the boundary between the LRR11 and LRR12 modules that is responsible for binding to ligands (*Jin et al., 2007*; *Kang et al., 2009*). In contrast, the asparagine ladder in

the ectodomain of TLR15 is intact, thus indicating that TLR15 possibly does not have the structural transition and also does not form a hydrophobic pocket in the middle of its ectodomain. Therefore, considering the large sequence and structural differences between TLR15 and the TLRs in family 1, TLR15 should be regarded as an individual family.

TLR15 is able to be activated through the cleavage of its ectodomain by secreted virulence-associated fungal and bacterial proteases, and also can be activated by the diacylated lipopeptide from *Mycoplasma synoviae* (*De Zoete et al., 2011*; *Oven et al., 2013*). However, the functional sites on the ectodomain of TLR15 are still unclear. We found a highly evolutionarily conserved region in the convex surface of TLR15 ectodomain by using the information of a large number of the known sequences. We infer that this highly evolutionarily conserved region is probably closely related to the function of TLR15. Interestingly, this highly evolutionarily conserved region in TLR15 ectodomain is located on the convex surface of LRR11 module, whereas the known ligand-binding regions of TLRs in family 1 are also located on the border between the LRR11 and LRR12 modules.

The TIR domains of TLRs are responsible for signal transduction in response to stimulation from pathogens. The formation of TIR domain complex is critical for receptor signaling. The TIR domain interactions mediate the oligomerization of receptor TIR domains, and also mediate the association between the receptor and adapter TIR domains (*Xu et al., 2000*). We predicted that there was quite strong interaction between TLR15 TIR domain and itself, suggesting that TLR15 may recruit downstream adaptor in the form of a homodimer. The formation of TLR15 TIR domain homodimers can be bolstered by the known ability to signal when only TLR15 is transfected into HEK293 cells (*Boyd et al., 2012*; *De Zoete et al., 2011*). In previous structural works, several TIR-dimer interaction modes have been proposed (*Jang & Park, 2014*; *Nyman et al., 2008*; *Xu et al., 2000*). The five residues in TLR2 TIR domain were verified to be functionally important for signaling (*Tao et al., 2002*). We found that their equivalent residues in TLR15 were involved in the predicted homodimerization of TIR domains. Also, these five residues are highly evolutionarily conserved among TLR15s. In particular, the previous study demonstrated that Pro681 in the BB-loop of TLR2 TIR domain (corresponding to Pro745 in chicken TLR15) mediated the interaction with adaptor MyD88 and further BB-loop was suggested to be the site of adaptor protein recruitment (*Xu et al., 2000*). The mutation of the equivalent residue in the BB-loop of human TLR10 TIR domain also affects the interaction with adaptor MyD88 (*Hasan et al., 2005*). Therefore, some residues on the interface of TLR15 TIR domain homodimer also probably participate in the interaction with downstream adapter.

Toll-like receptors are located directly on the host-pathogen interface and might undergo coevolutionary dynamics with their pathogenic counterparts. The *dN/dS* value showed that TLR15 was evolutionarily conserved, but many positively selected sites were still identified. The previous study identified 8 positively selected sites in the ectodomain among six TLR15 sequences through REL method (*Alcaide & Edwards, 2011*). We identified 27 robust positively selected sites among 57 full-length TLR15 sequences using four methods. These positively selected sites are mainly located on the ectodomain that is responsible for recognizing the ligands, and are possibly related to the function of TLR15. Therefore, the

fact that so many positively selected sites were identified shows that there are coevolutionary dynamics between TLR15 and their pathogenic counterparts.

CONCLUSIONS

In this study, we identified 57 completed TLR15 genes from a large number of avian and reptilian genomes. TLR15 is phylogenetically closely related to family 1. Unlike the TLRs in family 1 with the broken asparagine ladders in the middle, TLR15 ectodomain possesses an intact asparagine ladder. The convex surface of TLR15 ectodomain has a highly evolutionarily conserved region, which is probably related to the function of TLR15. We found that TLR15 TIR domains were able to form homodimers in silico. The major contributions to the homodimer interface of TLR15 TIR domains are made by residues from the BB-loops and αC-helixes. Twenty-seven sites under positive selection that are probably associated with function were detected for TLR15. Overall, these findings provide novel insights into the structural and evolutionary characterizations of TLR15.

ACKNOWLEDGEMENTS

We would like to thank Hui Fu, Jing Liu, and Jing Zhao for providing the useful suggestions on the manuscript.

ADDITIONAL INFORMATION AND DECLARATIONS

Funding

This work was supported in part by the National 973 Research Project (No. 2014CB542400) and National Natural Science Foundation of China (No. 81570454). The funders had no role in study design, data collection and analysis, decision to publish, or preparation of the manuscript.

Grant Disclosures

The following grant information was disclosed by the authors:
National 973 Research Project: 2014CB542400.
National Natural Science Foundation of China: 81570454.

Competing Interests

The authors declare there are no competing interests.

Author Contributions

- Jinlan Wang and Zheng Zhang conceived and designed the experiments, performed the experiments, analyzed the data, wrote the paper, prepared figures and/or tables, reviewed drafts of the paper.
- Fen Chang performed the experiments, analyzed the data.
- Deling Yin conceived and designed the experiments, reviewed drafts of the paper.

Data Availability

The following information was supplied regarding data availability:

The raw data has been supplied as Data S1.

Supplemental Information

Supplemental information for this article can be found online at http://dx.doi.org/10.7717/peerj.2079#supplemental-information.

REFERENCES

Abascal F, Zardoya R, Telford MJ. 2010. TranslatorX: multiple alignment of nucleotide sequences guided by amino acid translations. *Nucleic Acids Research* **38**:W7–W13 DOI 10.1093/nar/gkq291.

Akira S, Takeda K. 2004. Toll-like receptor signalling. *Nature Reviews Immunology* **4**:499–511 DOI 10.1038/nri1391.

Alcaide M, Edwards SV. 2011. Molecular evolution of the toll-like receptor multigene family in birds. *Molecular Biology and Evolution* **28**:1703–1715 DOI 10.1093/molbev/msq351.

Anisimova M, Gascuel O. 2006. Approximate likelihood-ratio test for branches: a fast, accurate, and powerful alternative. *Systematic Biology* **55**:539–552 DOI 10.1080/10635150600755453.

Ashkenazy H, Erez E, Martz E, Pupko T, Ben-Tal N. 2010. ConSurf 2010: calculating evolutionary conservation in sequence and structure of proteins and nucleic acids. *Nucleic Acids Research* **38**:W529–W533 DOI 10.1093/nar/gkq399.

Baspinar A, Cukuroglu E, Nussinov R, Keskin O, Gursoy A. 2014. PRISM: a web server and repository for prediction of protein-protein interactions and modeling their 3D complexes. *Nucleic Acids Research* **42**:W285–W289 DOI 10.1093/nar/gku397.

Benson DA, Cavanaugh M, Clark K, Karsch-Mizrachi I, Lipman DJ, Ostell J, Sayers EW. 2013. GenBank. *Nucleic Acids Research* **41**:D36–D42 DOI 10.1093/nar/gks1195.

Botos I, Segal DM, Davies DR. 2011. The structural biology of Toll-like receptors. *Structure* **19**:447–459 DOI 10.1016/j.str.2011.02.004.

Boyd AC, Peroval MY, Hammond JA, Prickett MD, Young JR, Smith AL. 2012. TLR15 is unique to avian and reptilian lineages and recognizes a yeast-derived agonist. *Journal of Immunology* **189**:4930–4938 DOI 10.4049/jimmunol.1101790.

Brownlie R, Zhu J, Allan B, Mutwiri GK, Babiuk LA, Potter A, Griebel P. 2009. Chicken TLR21 acts as a functional homologue to mammalian TLR9 in the recognition of CpG oligodeoxynucleotides. *Molecular Immunology* **46**:3163–3170 DOI 10.1016/j.molimm.2009.06.002.

Cunningham F, Amode MR, Barrell D, Beal K, Billis K, Brent S, Carvalho-Silva D, Clapham P, Coates G, Fitzgerald S, Gil L, Girón CG, Gordon L, Hourlier T, Hunt SE, Janacek SH, Johnson N, Juettemann T, Kähäri AK, Keenan S, Martin FJ, Maurel T, McLaren W, Murphy DN, Nag R, Overduin B, Parker A, Patricio M,

Perry E, Pignatelli M, Riat HS, Sheppard D, Taylor K, Thormann A, Vullo A, Wilder SP, Zadissa A, Aken BL, Birney E, Harrow J, Kinsella R, Muffato M, Ruffier M, Searle SMJ, Spudich G, Trevanion SJ, Yates A, Zerbino DR, Flicek P. 2015. Ensembl 2015. *Nucleic Acids Research* **43**:D662–D669 DOI 10.1093/nar/gku1010.

De Zoete MR, Bouwman LI, Keestra AM, Van Putten JP. 2011. Cleavage and activation of a Toll-like receptor by microbial proteases. *Proceedings of the National Academy of Sciences of the United States of America* **108**:4968–4973 DOI 10.1073/pnas.1018135108.

Delport W, Poon AF, Frost SD, Kosakovsky Pond SL. 2010. Datamonkey 2010: a suite of phylogenetic analysis tools for evolutionary biology. *Bioinformatics* **26**:2455–2457 DOI 10.1093/bioinformatics/btq429.

Guan Y, Ranoa DR, Jiang S, Mutha SK, Li X, Baudry J, Tapping RI. 2010. Human TLRs 10 and 1 share common mechanisms of innate immune sensing but not signaling. *Journal of Immunology* **184**:5094–5103 DOI 10.4049/jimmunol.0901888.

Guindon S, Dufayard JF, Lefort V, Anisimova M, Hordijk W, Gascuel O. 2010. New algorithms and methods to estimate maximum-likelihood phylogenies: assessing the performance of PhyML 3.0. *Systematic Biology* **59**:307–321 DOI 10.1093/sysbio/syq010.

Hasan U, Chaffois C, Gaillard C, Saulnier V, Merck E, Tancredi S, Guiet C, Briere F, Vlach J, Lebecque S, Trinchieri G, Bates EEM. 2005. Human TLR10 is a functional receptor, expressed by B cells and plasmacytoid dendritic cells, which activates gene transcription through MyD88. *The Journal of Immunology* **174**:2942–2950 DOI 10.4049/jimmunol.174.5.2942.

Heil F, Hemmi H, Hochrein H, Ampenberger F, Kirschning C, Akira S, Lipford G, Wagner H, Bauer S. 2004. Species-specific recognition of single-stranded RNA via toll-like receptor 7 and 8. *Science* **303**:1526–1529 DOI 10.1126/science.1093620.

Higgs R, Cormican P, Cahalane S, Allan B, Lloyd AT, Meade K, James T, Lynn DJ, Babiuk LA, O'Farrelly C. 2006. Induction of a novel chicken Toll-like receptor following *Salmonella enterica* serovar Typhimurium infection. *Infection and Immunity* **74**:1692–1698 DOI 10.1128/IAI.74.3.1692-1698.2006.

Hu Y, Chen WW, Liu HX, Shan YJ, Zhu CH, Li HF, Zou JM. 2016. Genetic differences in ChTLR15 gene polymorphism and expression involved in *Salmonella enterica* natural and artificial infection respectively, of Chinese native chicken breeds, with a focus on sexual dimorphism. *Avian Pathology* **45**:13–25 DOI 10.1080/03079457.2015.1110849.

Jang TH, Park HH. 2014. Crystal structure of TIR domain of TLR6 reveals novel dimeric interface of TIR–TIR interaction for toll-like receptor signaling pathway. *Journal of Molecular Biology* **426**:3305–3313 DOI 10.1016/j.jmb.2014.07.024.

Jin MS, Kim SE, Heo JY, Lee ME, Kim HM, Paik SG, Lee H, Lee JO. 2007. Crystal structure of the TLR1-TLR2 heterodimer induced by binding of a tri-acylated lipopeptide. *Cell* **130**:1071–1082 DOI 10.1016/j.cell.2007.09.008.

Kang JY, Lee JO. 2011. Structural biology of the Toll-like receptor family. *Annual Review of Biochemistry* **80**:917–941 DOI 10.1146/annurev-biochem-052909-141507.

Kang JY, Nan X, Jin MS, Youn SJ, Ryu YH, Mah S, Han SH, Lee H, Paik SG, Lee JO. 2009. Recognition of lipopeptide patterns by Toll-like receptor 2-Toll-like receptor 6 heterodimer. *Immunity* **31**:873–884 DOI 10.1016/j.immuni.2009.09.018.

Katoh K, Standley DM. 2013. MAFFT multiple sequence alignment software version 7: improvements in performance and usability. *Molecular Biology and Evolution* **30**:772–780 DOI 10.1093/molbev/mst010.

Keestra AM, De Zoete MR, Bouwman LI, Van Putten JP. 2010. Chicken TLR21 is an innate CpG DNA receptor distinct from mammalian TLR9. *Journal of Immunology* **185**:460–467 DOI 10.4049/jimmunol.0901921.

Koblansky AA, Jankovic D, Oh H, Hieny S, Sungnak W, Mathur R, Hayden MS, Akira S, Sher A, Ghosh S. 2013. Recognition of profilin by Toll-like receptor 12 is critical for host resistance to Toxoplasma gondii. *Immunity* **38**:119–130 DOI 10.1016/j.immuni.2012.09.016.

Kosakovsky Pond SL, Frost SD. 2005. Not so different after all: a comparison of methods for detecting amino acid sites under selection. *Molecular Biology and Evolution* **22**:1208–1222 DOI 10.1093/molbev/msi105.

Krogh A, Larsson B, Von Heijne G, Sonnhammer EL. 2001. Predicting transmembrane protein topology with a hidden Markov model: application to complete genomes. *Journal of Molecular Biology* **305**:567–580 DOI 10.1006/jmbi.2000.4315.

Le SQ, Gascuel O. 2008. An improved general amino acid replacement matrix. *Molecular Biology and Evolution* **25**:1307–1320 DOI 10.1093/molbev/msn067.

Letunic I, Doerks T, Bork P. 2015. SMART: recent updates, new developments and status in 2015. *Nucleic Acids Research* **43**:D257–D260 DOI 10.1093/nar/gku949.

Liu L, Botos I, Wang Y, Leonard JN, Shiloach J, Segal DM, Davies DR. 2008. Structural basis of toll-like receptor 3 signaling with double-stranded RNA. *Science* **320**:379–381 DOI 10.1126/science.1155406.

Matsuo A, Oshiumi H, Tsujita T, Mitani H, Kasai H, Yoshimizu M, Matsumoto M, Seya T. 2008. Teleost TLR22 recognizes RNA duplex to induce IFN and protect cells from birnaviruses. *Journal of Immunology* **181**:3474–3485 DOI 10.4049/jimmunol.181.5.3474.

Murrell B, Moola S, Mabona A, Weighill T, Sheward D, Kosakovsky Pond SL, Scheffler K. 2013. FUBAR: a fast, unconstrained bayesian approximation for inferring selection. *Molecular Biology and Evolution* **30**:1196–1205 DOI 10.1093/molbev/mst030.

Nyman T, Stenmark P, Flodin S, Johansson I, Hammarstrom M, Nordlund P. 2008. The crystal structure of the human toll-like receptor 10 cytoplasmic domain reveals a putative signaling dimer. *Journal of Biological Chemistry* **283**:11861–11865 DOI 10.1074/jbc.C800001200.

Offord V, Coffey TJ, Werling D. 2010. LRRfinder: a web application for the identification of leucine-rich repeats and an integrative Toll-like receptor database. *Developmental and Comparative Immunology* **34**:1035–1041 DOI 10.1016/j.dci.2010.05.004.

Ohto U, Shibata T, Tanji H, Ishida H, Krayukhina E, Uchiyama S, Miyake K, Shimizu T. 2015. Structural basis of CpG and inhibitory DNA recognition by Toll-like receptor 9. *Nature* **520**:702–705 DOI 10.1038/nature14138.

Oven I, Resman Rus K, Dusanic D, Bencina D, Keeler Jr CL, Narat M. 2013. Diacylated lipopeptide from Mycoplasma synoviae mediates TLR15 induced innate immune responses. *Veterinary Research* **44**:99 DOI 10.1186/1297-9716-44-99.

Park BS, Song DH, Kim HM, Choi BS, Lee H, Lee JO. 2009. The structural basis of lipopolysaccharide recognition by the TLR4-MD-2 complex. *Nature* **458**:1191–1195 DOI 10.1038/nature07830.

Petersen TN, Brunak S, Von Heijne G, Nielsen H. 2011. SignalP 4.0: discriminating signal peptides from transmembrane regions. *Nature Methods* **8**:785–786 DOI 10.1038/nmeth.1701.

Roach JC, Glusman G, Rowen L, Kaur A, Purcell MK, Smith KD, Hood LE, Aderem A. 2005. The evolution of vertebrate Toll-like receptors. *Proceedings of the National Academy of Sciences of the United States of America* **102**:9577–9582 DOI 10.1073/pnas.0502272102.

Shaughnessy RG, Meade KG, Cahalane S, Allan B, Reiman C, Callanan JJ, O'Farrelly C. 2009. Innate immune gene expression differentiates the early avian intestinal response between Salmonella and Campylobacter. *Veterinary Immunology and Immunopathology* **132**:191–198 DOI 10.1016/j.vetimm.2009.06.007.

Shi Z, Cai Z, Sanchez A, Zhang T, Wen S, Wang J, Yang J, Fu S, Zhang D. 2011. A novel Toll-like receptor that recognizes vesicular stomatitis virus. *Journal of Biological Chemistry* **286**:4517–4524 DOI 10.1074/jbc.M110.159590.

Tamura K, Stecher G, Peterson D, Filipski A, Kumar S. 2013. MEGA6: molecular evolutionary genetics analysis version 6.0. *Molecular Biology and Evolution* **30**:2725–2729 DOI 10.1093/molbev/mst197.

Tanji H, Ohto U, Shibata T, Taoka M, Yamauchi Y, Isobe T, Miyake K, Shimizu T. 2015. Toll-like receptor 8 senses degradation products of single-stranded RNA. *Nature Structural & Molecular Biology* **22**:109–115 DOI 10.1038/nsmb.2943.

Tao X, Xu Y, Zheng Y, Beg AA, Tong L. 2002. An extensively associated dimer in the structure of the C713S mutant of the TIR domain of human TLR2. *Biochemical and Biophysical Research Communications* **299**:216–221 DOI 10.1016/S0006-291X(02)02581-0.

Tuncbag N, Gursoy A, Nussinov R, Keskin O. 2011. Predicting protein-protein interactions on a proteome scale by matching evolutionary and structural similarities at interfaces using PRISM. *Nature Protocols* **6**:1341–1354 DOI 10.1038/nprot.2011.367.

Wang J, Zhang Z, Fu H, Zhang S, Liu J, Chang F, Li F, Zhao J, Yin D. 2015a. Structural and evolutionary characteristics of fish-specific TLR19. *Fish and Shellfish Immunology* **47**:271–279 DOI 10.1016/j.fsi.2015.09.005.

Wang J, Zhang Z, Liu J, Li F, Chang F, Fu H, Zhao J, Yin D. 2015b. Structural characterization and evolutionary analysis of fish-specific TLR27. *Fish and Shellfish Immunology* **45**:940–945 DOI 10.1016/j.fsi.2015.06.017.

Xu Y, Tao X, Shen B, Horng T, Medzhitov R, Manley JL, Tong L. 2000. Structural basis for signal transduction by the Toll/interleukin-1 receptor domains. *Nature* **408**:111–115 DOI 10.1038/35040600.

Yang J, Yan R, Roy A, Xu D, Poisson J, Zhang Y. 2015. The I-TASSER Suite: protein structure and function prediction. *Nature Methods* **12**:7–8 DOI 10.1038/nmeth.3213.

Yarovinsky F, Zhang D, Andersen JF, Bannenberg GL, Serhan CN, Hayden MS, Hieny S, Sutterwala FS, Flavell RA, Ghosh S, Sher A. 2005. TLR11 activation of dendritic cells by a protozoan profilin-like protein. *Science* **308**:1626–1629 DOI 10.1126/science.1109893.

Yeh DW, Liu YL, Lo YC, Yuh CH, Yu GY, Lo JF, Luo Y, Xiang R, Chuang TH. 2013. Toll-like receptor 9 and 21 have different ligand recognition profiles and cooperatively mediate activity of CpG-oligodeoxynucleotides in zebrafish. *Proceedings of the National Academy of Sciences of the United States of America* **110**:20711–20716 DOI 10.1073/pnas.1305273110.

Yoon SI, Kurnasov O, Natarajan V, Hong M, Gudkov AV, Osterman AL, Wilson IA. 2012. Structural basis of TLR5-flagellin recognition and signaling. *Science* **335**:859–864 DOI 10.1126/science.1215584.

Zhang G, Li C, Li Q, Li B, Larkin DM, Lee C, Storz JF, Antunes A, Greenwold MJ, Meredith RW, Ödeen A, Cui J, Zhou Q, Xu L, Pan H, Wang Z, Jin L, Zhang P, Hu H, Yang W, Hu J, Xiao J, Yang Z, Liu Y, Xie Q, Yu H, Lian J, Wen P, Zhang F, Li H, Zeng Y, Xiong Z, Liu S, Zhou L, Huang Z, An N, Wang J, Zheng Q, Xiong Y, Wang G, Wang B, Wang J, Fan Y, Da Fonseca RR, Alfaro-Núñez A, Schubert M, Orlando L, Mourier T, Howard JT, Ganapathy G, Pfenning A, Whitney O, Rivas MV, Hara E, Smith J, Farré M, Narayan J, Slavov G, Romanov MN, Borges R, Machado JP, Khan I, Springer MS, Gatesy J, Hoffmann FG, Opazo JC, Håstad O, Sawyer RH, Kim H, Kim K-W, Kim HJ, Cho S, Li N, Huang Y, Bruford MW, Zhan X, Dixon A, Bertelsen MF, Derryberry E, Warren W, Wilson RK, Li S, Ray DA, Green RE, OBrien SJ, Griffin D, Johnson WE, Haussler D, Ryder OA, Willerslev E, Graves GR, Alström P, Fjeldså J, Mindell DP, Edwards SV, Braun EL, Rahbek C, Burt DW, Houde P, Zhang Y, Yang H, Wang J, Consortium AG, Jarvis ED, Gilbert MTP, Wang J. 2014. Comparative genomics reveals insights into avian genome evolution and adaptation. *Science* **346**:1311–1320 DOI 10.1126/science.1251385.